Supplementary figure 1

A

	GO biological process	No. of genes	Adj. P-val.
1	Organic acid metabolic process	36	6.74×10^{-19}
	Oxoacid metabolic process	30	1.86×10^{-13}
	Organic anion transport	19	6.92×10^{-11}
	Anion transport	21	1.65×10^{-10}
2	Response to oxygen-containing compounds	48	8.21×10^{-20}
	Inflammatory response	30	5.30×10^{-15}
	Response to wounding	30	7.27×10^{-12}
3	Collagen metabolic process	5	6.19×10^{-5}
	Extracellular matrix organization	6	3.57×10^{-4}
4	Immune response	20	1.01×10^{-14}
	Regulation of lymphocyte activation	10	2.06×10^{-8}

B

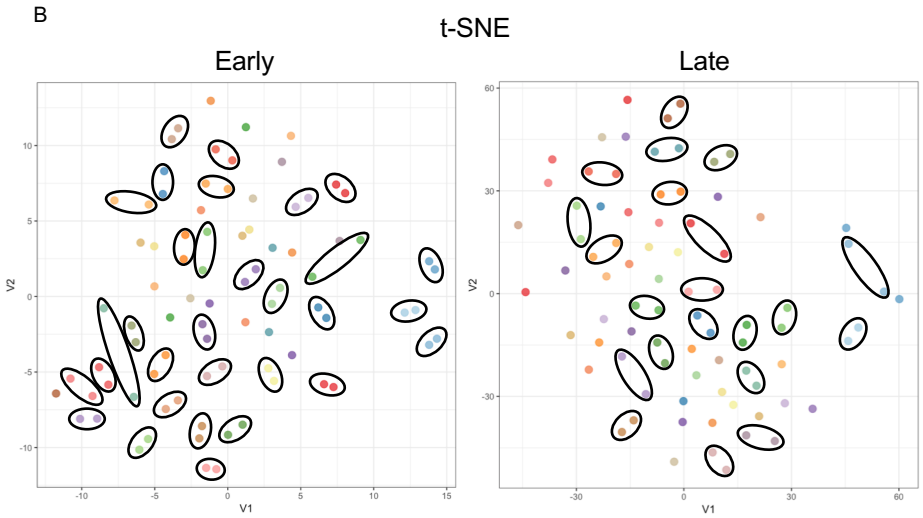

C

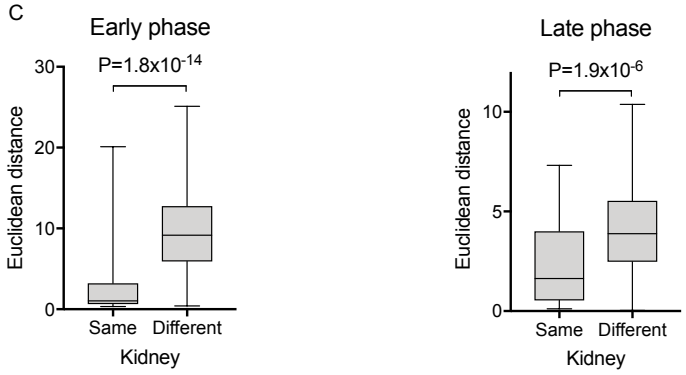

Suppl. figure 1. Intraindividual transcriptome variability

(A) Gene Ontology (GO) analysis on genes showing a high level of correlation among the 500 most variable genes in RNAseq data from all 163 protocol biopsies, as reported in Figure 1A. The number of genes and adjusted P values (Benjamini-Hochberg) are shown for the most significantly enriched terms (biological process) for each cluster. (B) t-distributed stochastic neighbor embedding (t-SNE) analysis on RNAseq data, including samples of the early (left panel; samples collected before implantation and after implantation – PRE and POST) or the late phase (right panel; samples collected 3 months and 12 months after transplantation – 3M, 12M). Samples from the same patients are shown in the same color within each panel and are included in a circle if clustered together. (C) Box plots of the Euclidian distance between the points in the t-SNE analysis shown in (B) comparing the distance between the points from the same and from different kidneys, as indicated. The Euclidian distances between samples from the same patient and from different patients were compared by unpaired single-sided t test.

Supplementary figure 2

A

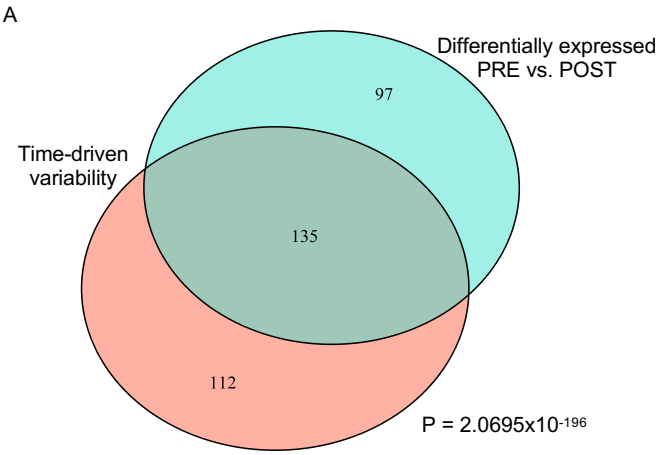

B

GO biological process	No. of genes	Adj. P-val.
Response to oxygen-containing compound	60	6.35×10^{-17}
Regulation of cell death	58	2.49×10^{-15}
Regulation of apoptotic process	55	4.72×10^{-15}

Suppl. figure 2. Time-driven variance and early response to ischemia reperfusion
(A) Venn diagram showing the overlap between the genes differentially expressed in POST (compared to PRE, i.e. samples collected after and before implantation, respectively) and genes displaying a time-dependent variance (as shown in Figure 1C). Significance of enrichment was determined by hypergeometric test. (B) Gene Ontology (GO) analysis on genes displaying a time-driven variance (as shown in Figure 1C). The number of genes and adjusted P values (Benjamini-Hochberg) are shown for the most significantly enriched terms (biological process).

Supplementary figure 3

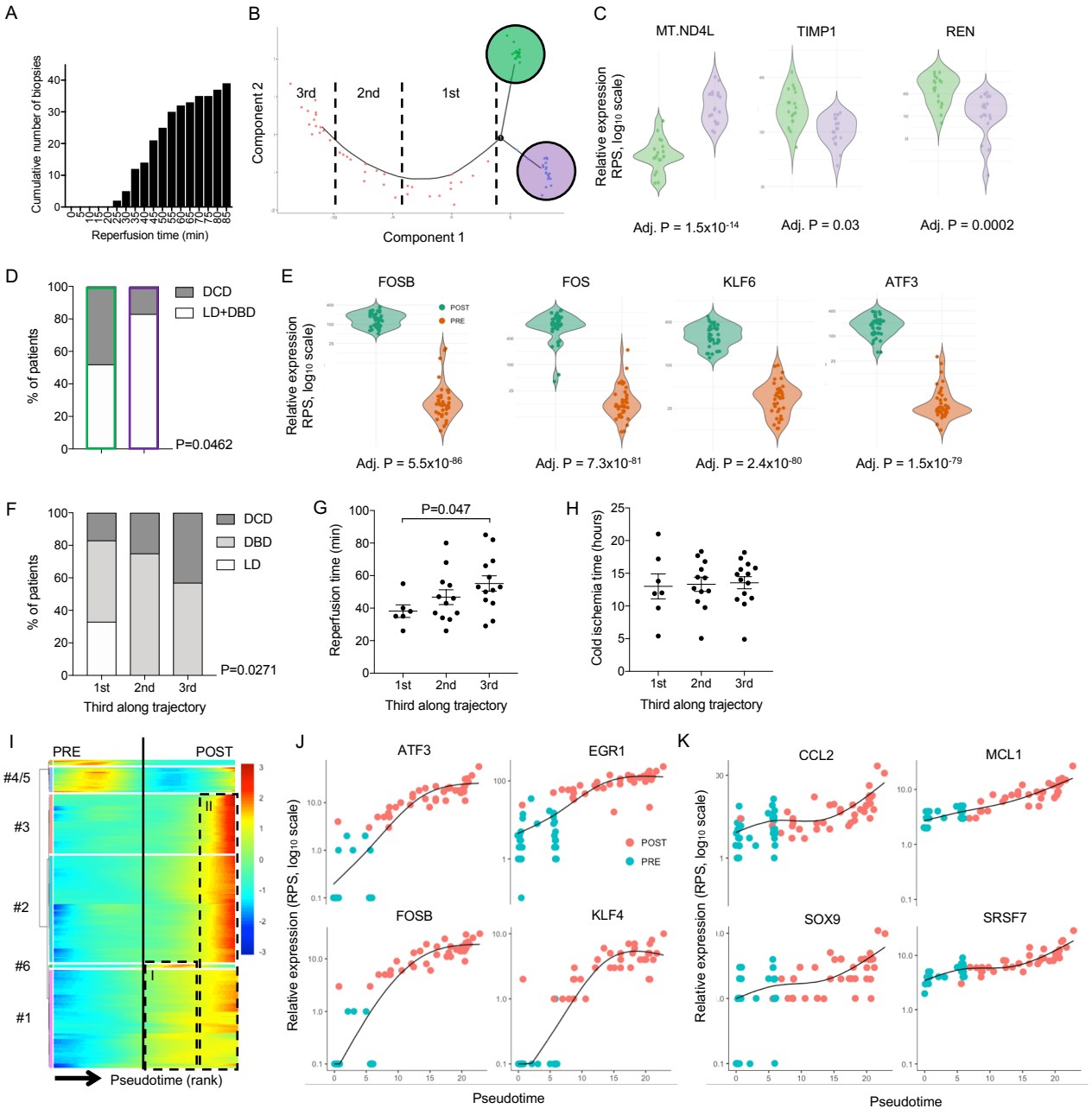

Suppl. Figure 3. Early response to ischemia reperfusion injury.
Histograms indicating the cumulative reperfusion time distribution, i.e. time between kidney reperfusion and collection of the post-implantation biopsy (POST), according to clinical records. (B) Identification of groups of interest in the early pseudotime analysis (s. Figure 2A): pre-implantation biopsies (PRE) were separated in two groups by the Monocle algorithm (green and purple), the trajectory including the POST samples was divided in equal thirds based on the pseudotime values. (C) Violin plots showing representative examples of relative expression in mRNA per sample (RPS) in genes differentially expressed in the two PRE groups, as shown in panel B (N=38). Adjusted P values are reported (Benjamini-Hochberg). (D) Histogram showing the % of donors after cardiac death (DCD) in each PRE group, as defined in panel B. The groups were compared by Chi-square test, N=38. (E) Violin plots of the top 4 up-regulated genes in POST compared to PRE samples. Adjusted P values are reported (Benjamini-Hochberg), N=77. (F) Histogram showing the % of donor type in each third of the POST trajectory (DBD: donor after brain death, LD: living donor). The groups were compared by Chi-square test, N=38. (G-H) Reperfusion time and cold-ischemia time in each third of the POST trajectory, as defined in panel B. The groups were compared by Mann Whithney test, N=37. (I) Cluster analysis of all genes differentially expressed along the pseudotime presented in Figure 2A: samples are aligned from left to right according to the order shown in Figure 2A. Genes are vertically aligned and classified in clusters as indicated on the left. The colors indicate the relative expression of the genes. The time of reperfusion is indicated by the solid vertical line. I and II indicate the 2 waves of genes up-regulated after reperfusion. The complete list of genes is presented in the suppl. materials (J-K) Representative examples of genes upregulated in the first (J) and in the second (K) wave of transcriptional regulation after reperfusion.

Supplementary figure 4

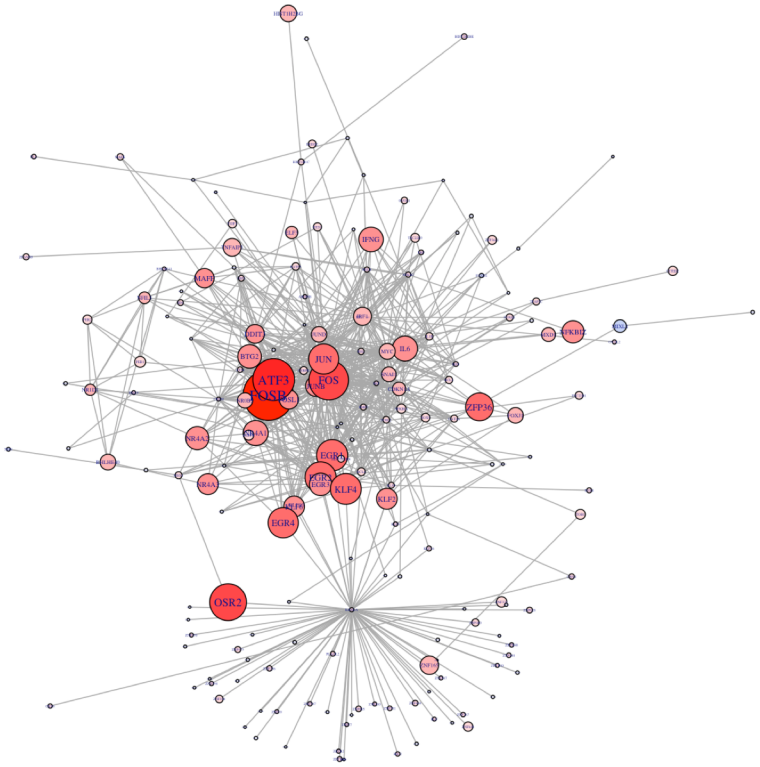

Suppl. figure 4. Network analysis.
Kamada Kawai plot (igraph network visualization) of the transcription factor centered gene network analysis based on differentially expressed genes between pre- and post-implantation samples. The size of the vertices correlates with the absolute value of log fold change. Red indicates upregulated after reperfusion. The top 200 genes are shown.

Supplementary figure 5

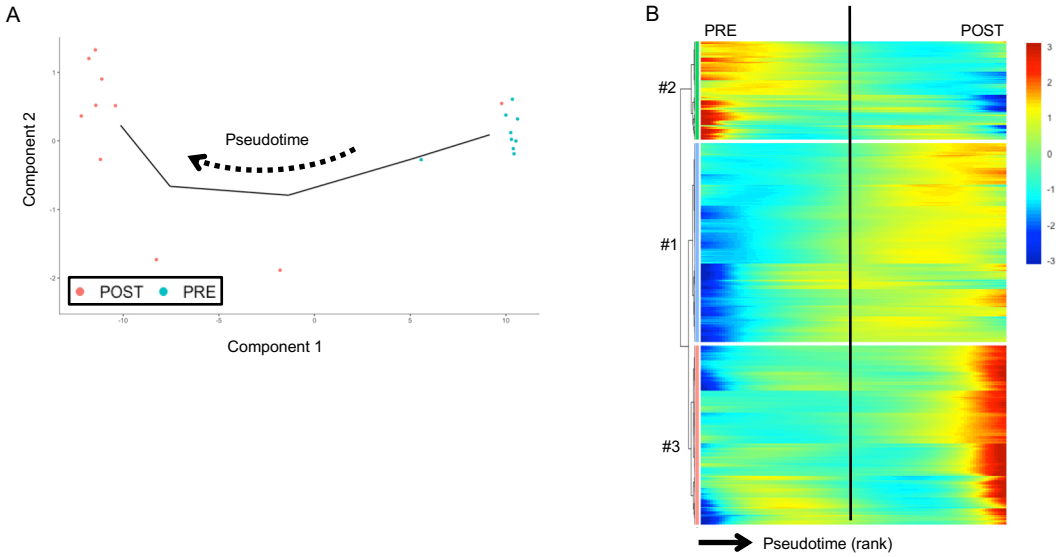

Suppl. figure 5. Early response to ischemia reperfusion in the human liver.
Pseudotime analysis including samples collected before (PRE, N=10) and after liver implantation (POST, N=10). (A) Sample state ordering in the reduced dimensional space, as determined by the Monocle algorithm. (B) Cluster analysis of all genes differentially expressed along the pseudotime presented in (A). Samples are aligned from left to right according to the order shown in (A). Genes are vertically aligned and classified in clusters as indicated on the left (the list of genes is presented in the supplementary materials). The colors indicate the relative expression of the genes.

Supplementary figure 6

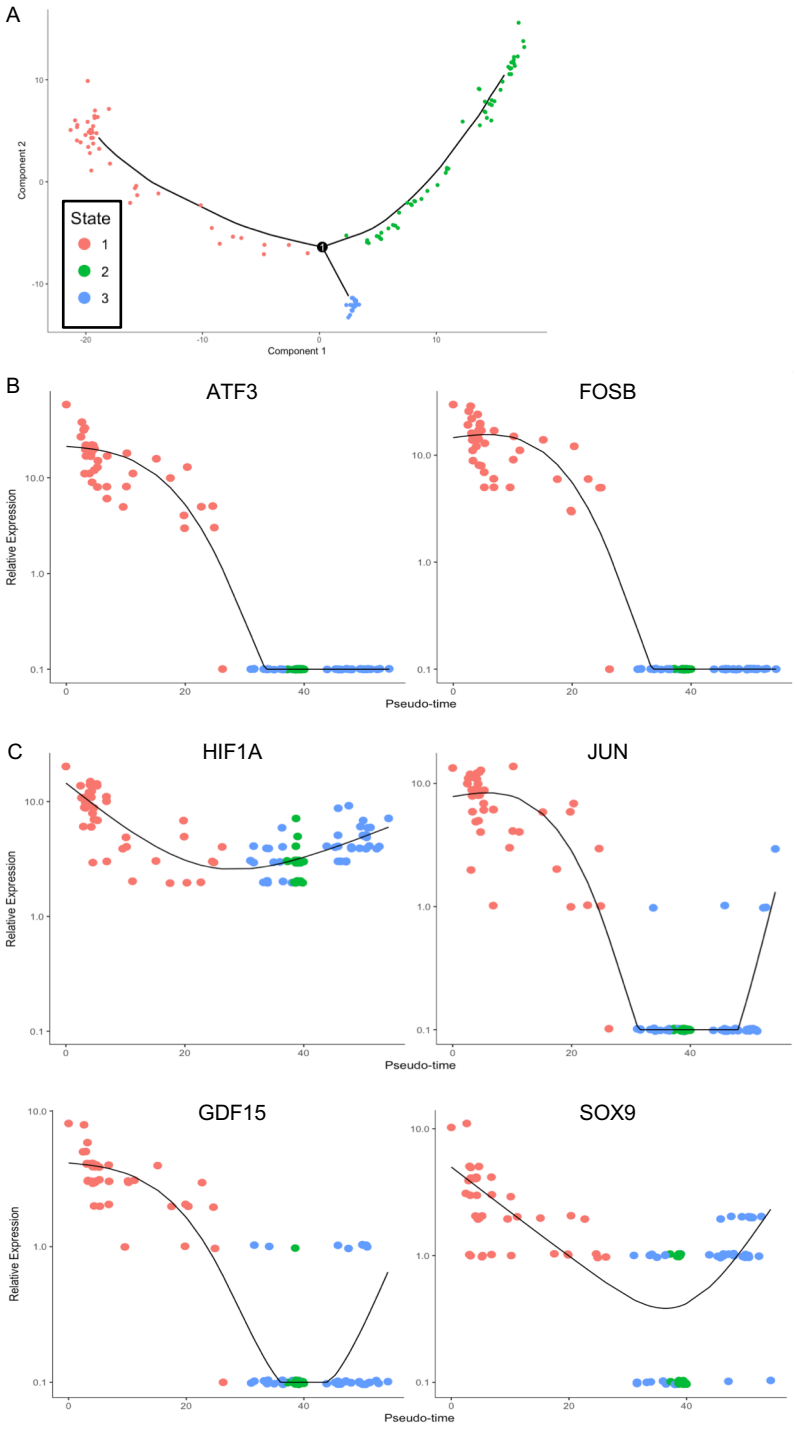

Suppl. figure 6. Late regulation of genes involved in the early response to ischemia/reperfusion injury.
(A) Pseudotime analysis as reported in Figure 3C, indicating the 3 states identified by the Monocle algorithm (shown here as a reference for the interpretation of the following plots). (B-C) Representative examples of the relative expression of early response genes along the pseudotime. All early-response genes were strongly up-regulated in the after implantation (POST, in red); some genes were consistently low at 3 and 12 months (B), whereas another set of genes was up-regulated in the late phases of the transition to fibrosis (C).